Chapter 6

Brownian Dynamics

Contents

In 1827 the botanist Robert Brown examined under his microspcope pollen of plants suspended in water. He observed that the pollen, about 10^{-6}m in diameter, performed stochastic motions of the order of 10^{-5}m. Even though Brown could not explain the cause of this motion any continuous stochastic process like that of a pollen is now referred to as *Brownian dynamics*.

In this chapter we introduce a numerical technique that generates a solution of the Fokker-Planck equation (5.1) by simulating an ensemble of stochastic processes. Due to these stochastic processes one calls this numerical method *Brownian dynamics* as well.

We provide two derivations of the numerical method of Brownian dynamics. In the first section we transform the Fokker-Planck equation (5.1) into a multi-dimensional integral. We then explain in the second section how to evaluate this multi-dimensional integral using the Monte Carlo integration method introduced in the previous chapter. We show in the third section that this Monte Carlo integration is equivalent to simulating an ensemble of stochastic processes. The equivalence is shown by deriving the Brownian dynamics method a second time starting with the stochastic differential equation (5.2). We examplify the idea of Brownian dynamics by applying it to a free diffusion model in the fourth section and conclude this chapter in the fifth section by showing how to incorporate boundary conditions in Brownian dynamics.

6.1   Discretization of Time

Discretization is the basis of many numerical procedures. This also holds true for Brownian dynamics. The object of discretization is the continuous time axis. A computer can not represent a continuous line or function. The infinitely many points would simply not fit into a finite digital computer nor could they be processed in a finite amount of time. Hence, one needs to approximate a continuous dimension with a finite set of points. This approximation is called discretization.

We solve the Fokker-Planck equation numerically by breaking the time axes paramerized by t into discrete points labeled by $t_0, t_1, t_2, \ldots$. These time points do not need to be equally spaced, but they usually are to simplfy the calculations.

One now has to adapt the Fokker-Planck equation (2.148) to the discretized time axis. For the sake of simplicity we consider the one-dimensional version

$$\partial_t \, p(x,t|x_0,t_0) \;\; = \;\; -\partial_x \, A(x,t) \, p(x,t|x_0,t_0) \, + \, \frac{1}{2} \, \partial_x^2 \, B^2(x,t) \, p(x,t|x_0,t_0) \; . \tag{6.1}$$

Let $p(x,t|x_0,t_0)$ be the, yet unknown, solution of (6.1) for the initial condition $x(t_0) = x_0$. One finds a solution $p(x,t|x_0,t_0)$ on a discrete sequence of times $\{t_0, t_1, t_2, \ldots\}$ by constructiong transition probabilities $p(x_{i+1},t_{i+1}|x_i,t_i)$ from one discrete time point t_i to the next. With these transition probabilities one can reassemble the complete solution $p(x,t|x_0,t_0)$.

We need to first disassemble the time evolution of $p(x,t|x_0,t_0)$ into many small time increments. For this purpose we proceed as follows. To obtain a solution $p(x_2,t_2|x_0,t_0)$ with an initial starting position at $x(t_0) = x_0$ one can first solve for $p(x_1,t_1|x_0,t_0)$ which describes the solution for an intermediate state at some time t_1 prior to t_2 and after t_0. The probability distribution at time t_1 may then be taken as the initial condition for a second solution of (6.1) reaching from time t_1 to time t_2. This second solution can be assembled due to the linearity of (6.1) using $p(x_2,t_2|x_1,t_1)$ for the initial condition $x(t_1) = x_1$. Summing $p(x_2,t_2|x_1,t_1)$ over all possible initial positions x_1 in the domain Ω weighted with the initial probability determined through $p(x_1,t_1|x_0,t_0)$ one obtains $p(x_2,t_2|x_0,t_0)$ and the Chapman Kolmogorow equation

$$p(x_2,t_2|x_0,t_0) \;\; = \;\; \int_\Omega dx_1 \; p(x_2,t_2|x_1,t_1) \, p(x_1,t_1|x_0,t_0) \; . \tag{6.2}$$

This is the Chapman-Kolmogorov equation encountered already above [c.f. (9.17)]. The process of dividing the evolution in the interval $[t_0,t_2]$ into consecutive evolution in the intervals $[t_0,t_1]$ and $[t_1,t_2]$ can be repeated. For this purpose one starts from (6.2), replaces variables x_2 and t_2 with x_3 and t_3, and applies (6.2) to $p(x_3,t_3|x_1,t_1)$ while naming the intermediate state x_2 and t_2. One derives

$$\begin{aligned} p(x_3,t_3|x_0,t_0) \;\; &= \;\; \int_\Omega dx_1 \; p(x_3,t_3|x_1,t_1) \, p(x_1,t_1|x_0,t_0) \\ &= \;\; \iint_\Omega dx_2 \, dx_1 \; p(x_3,t_3|x_2,t_2) \, p(x_2,t_2|x_1,t_1) \, p(x_1,t_1|x_0,t_0) \; . \end{aligned} \tag{6.3}$$

These steps may be repeated again. Doing so $(N-1)$-times one obtains

$$p(x_N,t_N|x_0,t_0) \;\; = \;\; \underbrace{\int \cdots \int_\Omega}_{(N-1)\,\text{times}} \left(\prod_{i=1}^{N-1} dx_i \; p(x_{i+1},t_{i+1}|x_i,t_i) \right) p(x_1,t_1|x_0,t_0) \; . \tag{6.4}$$

The procedure above has divided now the time evolution of $p(x_N,t_N|x_0,t_0)$ into N steps over time intervals $[t_{i+1},t_i]$ where t_i, $i = 1, 2, \ldots, N-1$ denotes the intermediate times. We will identify below t and t_N. In order to evaluate $p(x_N,t_N|x_0,t_0)$ we need to determine the transition probabilities $p(x_{i+1},t_{i+1}|x_i,t_i)$. The respective algorithm can exploit the possibility that one can choose the time intervals $[t_{i+1},t_i]$ very short such that certain approximations can be envoked without undue errors. In fact, for equally spaced time points t_i the length of each time segment is $\Delta t = (t_i - t_{i-1}) = (t - t_0)/N$. One can choose N always large enough that the time period Δt is short enough to justify the approximations introduced below.

Let Δx be the typical distance that a particle governed by the probability distribution $p(x, t_0 + \Delta t | x_0, t_0)$ may cover due to drift and diffusion within a time period Δt, i.e.

$$
\begin{aligned}
\Delta x &= \left| \langle\!\langle x \rangle\!\rangle \right| + \sqrt{\langle\!\langle x^2 \rangle\!\rangle} \\
&\sim \left| A(x_0, t_0) \right| \Delta t + B(x_0, t_0) \sqrt{\Delta t} .
\end{aligned}
\tag{6.5}
$$

The approximation introduced assumes that $A(x, t)$ and $B(x, t)$ are constant for each time period $[t_i, t_{i+1}]$ and spatially independent in each range $[x_i - \Delta x, x_i + \Delta x]$,

$$
\begin{aligned}
A\big(t \in [t_i, t_{i+1}], x \in [x_i - \Delta x, x_i + \Delta x]\big) &\sim A(t_i, x_i) \tag{6.6} \\
B\big(t \in [t_i, t_{i+1}], x \in [x_i - \Delta x, x_i + \Delta x]\big) &\sim B(t_i, x_i) , \tag{6.7}
\end{aligned}
$$

One replaces than the functions $p(x_{i+1}, t_{i+1} | x_i, t_i)$ in (6.4) by solutions of the Fokker-Planck equation (6.1) with constant coefficients $A(x, t)$ and $B(x, t)$. In case of boundary conditions at $x \to \pm\infty$ the resulting expression is, according to (4.28, 4.39)

$$
\begin{aligned}
p(x_{i+1}, &t_{i+1} | x_i, t_i) = \\
&\frac{1}{\sqrt{2\pi\, B^2(x_i, t_i)\,(t_{i+1} - t_i)}} \; \exp\left(-\frac{\big(x_{i+1} - x_i - A(x_i, t_i)\,(t_{i+1} - t_i)\big)^2}{2\, B^2(x_i, t_i)\,(t_{i+1} - t_i)} \right) .
\end{aligned}
\tag{6.8}
$$

We will consider solutions for other boundary conditions on page 100 further below.
Employing (6.8) in the iterated form of the Chapman-Kolmogorow equation (6.4), one derives

$$
p(x, t | x_0, t_0) = \tag{6.9}
$$
$$
\underbrace{\int \cdots \int_{\Omega}}_{(N-1)\,\text{times}} \left(\prod_{i=1}^{N-1} dx_i \right) \prod_{i=0}^{N-1} \frac{1}{\sqrt{2\pi\, B^2(x_i, t_i)\,\Delta t}} \; \exp\left(-\frac{\big(x_{i+1} - x_i - A(x_i, t_i)\,\Delta t\big)^2}{2\, B^2(x_i, t_i)\,\Delta t} \right) .
$$

Thus, we have solved the Fokker-Planck equation (6.1) up to an N-dimensional integral. This integral needs to be evaluated numerically for which purpose one applies the Monte Carlo integration method.

6.2 Monte Carlo Integration of Stochastic Processes

The integral on the r.h.s. of (6.4) and (6.9) is a truely high-dimensional integral. The Monte Carlo method is therefore the appropriate integration method.
Before we apply the Monte Carlo method we modify equation (6.4) slightly. The probability distribution $p(x, t | x_0, t_0)$ is not always what one wants to determine. A more feasible construct is the average $\bar{q}(t | x_0, t_0)$ of an arbitrary observable Q with a sensitivity function $q(x)$ in state space Ω given by the integral

$$
\bar{q}(t | x_0, t_0) = \int_{\Omega} dx\; q(x)\, p(x, t | x_0, t_0) . \tag{6.10}
$$

Equation (6.10) is very comprehensive. Even the probability distribution $p(\tilde{x}, t | x_0, t_0)$ can be viewed as an observable Q, namely, for the sensitivity function $q_{\tilde{x}}(x) = \delta(x - \tilde{x})$.

We now apply the Monte Carlo integration method as stated in equation (5.26) to the expanded form of (6.10)

$$\bar{q}(t|x_0, t_0) = \int_\Omega dx \; q(x) \times \tag{6.11}$$

$$\underbrace{\int \cdots \int_\Omega}_{(N-1)\,\text{times}} \left(\prod_{i=1}^{N-1} dx_i \; p(x_{i+1}, t_{i+1}|x_i, t_i) \right) p(x_1, t_1|x_0, t_0) \; .$$

One can associate $q(x)$ with $f(\boldsymbol{x})$ and the product of $p(x_{i+1}, t_{i+1}|x_i, t_i)$ with $p(\boldsymbol{x})$. The only problem now is finding a random number generator that produces random numbers $\tilde{r}$ with a distribution equivalent to the product of all $p(x_{i+1}, t_{i+1}|x_i, t_i)$. This seems to be an impossible endeavor unless one recalls how the product of all the $p(x_{i+1}, t_{i+1}|x_i, t_i)$ came about.

Let us start with the case $N = 0$. Given a random number generator that produces numbers $\tilde{r}(x_0, t_0)$ with a distribution $p(x, t|x_0, t_0)$ the solution is

$$\bar{q}(t|x_0, t_0) = \int_\Omega dx \; q(x) \, p(x, t|x_0, t_0)$$

$$\sim \frac{1}{M} \sum_{k=1}^M q(\tilde{r}_k(x_0, t_0)) \; . \tag{6.12}$$

We denote the x_0 and t_0-dependence of the random numbers $\tilde{r}_k(x_0, t_0)$ explicitly for later use. The reader should note that $\tilde{r}_k(x_0, t_0)$ exhibits a distribution $p(x, t|x_0, t_0)$ around x_0.

Implementing the Chapman-Kolmogorov equation (6.2) for $p(x, t|x_0, t_0)$ once we obtain the case $N = 1$ and two nested integrals.

$$\bar{q}(t|x_0, t_0) = \int_\Omega dx \; q(x) \int_\Omega dx_1 \; p(x, t|x_1, t_1) \, p(x_1, t_1|x_0, t_0) \; . \tag{6.13}$$

To approximate (6.13) numerically one determines first the inner integral with the integration variable x_1. The Monte Carlo method yields

$$\bar{q}(t|x_0, t_0) \sim \int_\Omega dx \; q(x) \frac{1}{M} \sum_{k_0=1}^M p(x, t|r_{k_0}(x_0, t_0), t_1) \; . \tag{6.14}$$

In a second step one applies applies the Monte Carlo method to the outer integral, now however with a probability distribution $p(x, t|\tilde{r}_{k_0}(x_0, t_0), t_1)$ exhibiting the inital starting point $\tilde{r}_{k_1}(x_0, t_0)$. We therefore use the random numbers $\tilde{r}_{k_1}(\tilde{r}_{k_0}(x_0, t_0), t_1)$.

$$\bar{q}(t|x_0, t_0) \sim \frac{1}{M^2} \sum_{k_1=1}^M \sum_{k_0=1}^M q(\tilde{r}_{k_1}(\tilde{r}_{k_0}(x_0, t_0), t_1)) \; . \tag{6.15}$$

Note the nesting of random numbers $\tilde{r}_{k_1}(\tilde{r}_{k_0}(x_0, t_0), t_1)$. The Gaussian random number $\tilde{r}_{k_1}(\dots)$ is distributed around the previous random number $\tilde{r}_{k_0}(\dots)$ which itself is distributed around x_0.

Performing the above steps N times, thus iterating the Chapman-Kolmogorov equation (6.9), one

obtains

$$
\begin{aligned}
\bar{q}(t|x_0,t_0) &= \int_\Omega dx\, q(x) \underbrace{\int \cdots \int_\Omega}_{(N-1)\,\text{times}} \left(\prod_{i=1}^{N-1} dx_i\, p(x_{i+1},t_{i+1}|x_i,t_i) \right) p(x_1,t_1|x_0,t_0) \\
&\sim \frac{1}{M^N} \sum_{k_0=1}^{M} \sum_{k_1=1}^{M} \cdots \sum_{k_N=1}^{M} q(\tilde{r}_{k_N}(\ldots \tilde{r}_{k_1}(\tilde{r}_{k_0}(x_0,t_0),t_1)\ldots,t_N))\,,
\end{aligned}
\tag{6.16}
$$

where the random numbers $\tilde{r}_{k_j}(x_j,t_j)$ should exhibit the probability distributions

$$
p\big(\tilde{r}_{k_j}(x_j,t_j)\big) = p(x_{j+1}t_{j+1}|x_j,t_j)\,.
\tag{6.17}
$$

The iteration above simplifies the problem of finding an appropriate random number generator. We now need random numbers that simply obey (6.17). In the specific case (6.8) one can generate the appropriate random numbers $\tilde{r}_k(x_0,t_0)$ utilizing a Gaussian number generator as described in the previous chapter. If r_k is a random number with the normalized Gaussian probability distribution $\exp(-r^2/2)/\sqrt{2\pi}\, dr$ one obtains $\tilde{r}_k(x_0,t_0)$ with the mapping

$$
\tilde{r}_k(x_0,t_0) = B(x_0,t_0)\sqrt{t-t_0}\, r_k + A(x_0,t_0)\,(t-t_0) + x_0\,.
\tag{6.18}
$$

With the help of (5.18) one can verify

$$
p(\tilde{r}(x_0,t_0)) = \frac{1}{\sqrt{2\pi\, B^2(x_0,t_0)\,(t-t_0)}} \exp\left(-\frac{\big(\tilde{r}(x_0,t_0) - x_0 - A(x_0,t_0)\,(t-t_0)\big)^2}{2\, B^2(x_0,t_0)\,(t-t_0)} \right)\,.
\tag{6.19}
$$

Thus, we finally have all the ingredients to perform the Monte Carlo integration (6.16). However, before putting (6.16) to use we can simplify the summations. The nesting of random numbers $\tilde{r}_{k_N}(\ldots \tilde{r}_{k_1}(\tilde{r}_{k_0}(x_0,t_0),t_1)\ldots,t_N)$ is in effect a random walk starting at x_0 and proceeding with Gaussian random steps $\tilde{r}_{k_i}$. With the summations in (6.16) one takes the average over all random walks that can be formed with a given set of M random steps $\tilde{r}_{k_i}$ for $i=1,\ldots,N$. One can simplify this equation by summing over M^N independent random pathes $\tilde{r}_{l_N}(\ldots \tilde{r}_{l_1}(\tilde{r}_{l_0}(x_0,t_0),t_1)\ldots,t_N)$ instead. Equation (6.16) becomes

$$
\bar{q}(t|x_0,t_0) \sim \frac{1}{M^N} \sum_{l=1}^{M^N} q(\tilde{r}_{l_N}(\ldots \tilde{r}_{l_1}(\tilde{r}_{l_0}(x_0,t_0),t_1)\ldots,t_N))\,.
\tag{6.20}
$$

6.3   Ito Calculus and Brownian Dynamics

Before applying Brownian dynamics in the form of equation (6.20) we want to shed light on the close relation between the Monte Carlo integration introduced above and the concept of stochastic processes as described in chapter 2.

Equation (6.20) describes the algorithm of Brownian dynamics. In essence one simulates the random walk of a given number of Brownian particles and samples their final position in state space Ω. To demonstrate this we return to chapter 2. Within the framework of Ito calculus we consider the stochastic differential equation (2.138) that corresponds to the Fokker-Planck equation (6.1)

$$
\partial_t\, x(t) = A(x(t),t) + B(x(t),t)\, \eta(t)\,.
\tag{6.21}
$$

The corresponding Ito-formula (2.137) is

$$
\begin{aligned}
df[x(t)] \;=\;& A(x(t),t)\Big(\partial_x\, f[x(t)]\Big)\, dt \;+\; B(x(t),t)\Big(\partial_x\, f[x(t)]\Big)\, d\omega(t) \\
& +\; \frac{1}{2}\, B^2(x(t),t)\left(\partial_x^2\, f[x(t)]\right) dt\ .
\end{aligned}
\tag{6.22}
$$

Assume $f[x(t)] = x(t)$. We thus derive for $x(t)$

$$
dx(t) \;=\; A(x(t),t)\, dt \;+\; B(x(t),t)\, d\omega(t)\ .
\tag{6.23}
$$

Integrating (6.23) over small time periods Δt for which we can assume $A(x(t),t)$ and $B(x(t),t)$ to be constant we obtain the finite difference equation

$$
x(t+\Delta t) - x(t) \;=\; A(x(t),t)\, \Delta t \;+\; B(x(t),t)\, \Delta\omega\ ,
\tag{6.24}
$$

with $\Delta\omega$ being a random variable with the Gaussian probability distribution (2.48) for $D = 1/2$. Such a random variable can be generated with a normalized Gaussian random number r and the mapping $\Delta\omega = \sqrt{\Delta t}\, r$

$$
x(t+\Delta t) - x(t) \;=\; A(x(t),t)\, \Delta t \;+\; B(x(t),t)\, \sqrt{\Delta t}\, r\ .
\tag{6.25}
$$

Note, that $x(t+\Delta t) - x(t)$ in (6.25) is the same as $\tilde{r}(x_0,t) - x_0$ defined in (6.18). Iterating equation (6.25) and thus numerically integrating the stochastic differential equation (6.21) according to Ito calculus, we generate a sample path $x(t)$ starting at any given $x(t_0) = x_0$. Such a sample path can then be used in the Monte Carlo procedure (6.20).

6.4   Free Diffusion

We now test the numerical Brownian dynamics procedure outlined above. For this purpose we resort to examples that can be solved analytically.

We begin with free diffusion in an infinite domain. The Fokker Planck equation, i.e., the respectively Einstein diffusion equation, is

$$
\partial_t\, p(x,t|x_0,t_0) \;=\; D\, \partial_x^2\, p(x,t|x_0,t_0)\ .
\tag{6.26}
$$

Comparing (6.26) and (6.1) one finds the drift coefficient $A(x,t)$ to be zero and the noise coupling coefficient $B(x,t) = \sqrt{2\,D}$ to be constant in time and space. Thus, assumptions (6.6) and (6.7) are met for any time step size $\Delta t = t_{i+1} - t_i$. Due to this fact one could choose $\Delta t = t - t_0$ and obtain with (6.8) the final result right away, thereby, rendering the following numerical simulation, employing a division into many short time intervals, unneccessary. Since we intend to verify the numerical approach we choose a division into N intermediate time steps nevertheless. These intermediate steps will become necessary when considering a potential and consequently a spatially dependent $A(x,t)$ further below.

One can proceed in a straight forward manner. Starting with Gaussian random numbers r_k as generated in (5.23) one derives the required random numbers $\tilde{r}_k(x,t)$ according to (6.18).

$$
\tilde{r}_k(x,t) \;=\; \sqrt{2\,D\,\Delta t}\, r_k \;+\; x.
\tag{6.27}
$$

These random numbers $\tilde{r}_k(x,t)$ exhibit the probability distribution

$$
p(\tilde{r}(x,t)) \;=\; \frac{1}{\sqrt{4\pi\, D\,\Delta t}}\, \exp\left(-\frac{\big(\tilde{r}(x,t)-x\big)^2}{4\,D\,\Delta t}\right)\ .
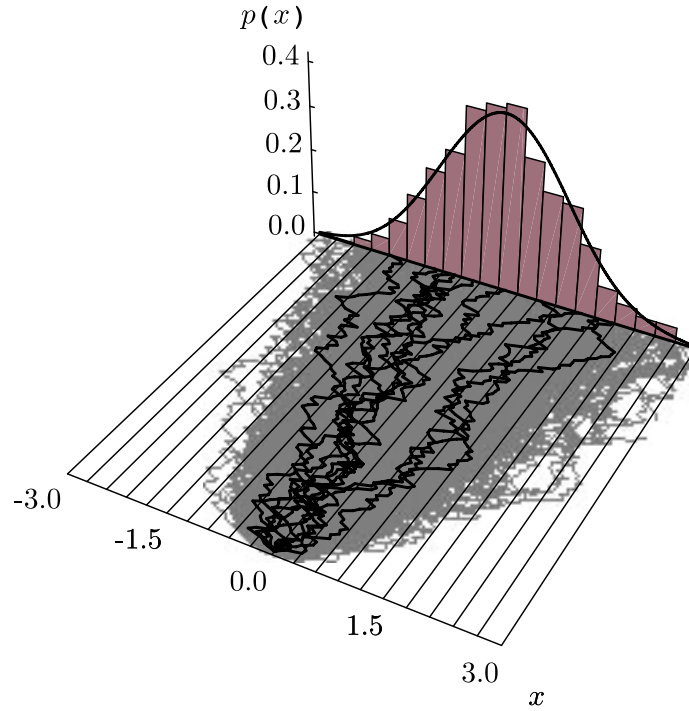\tag{6.28}
$$

$$p(x)$$

Figure 6.1: 1000 random trajectories generated by a Brownian dynamics simulation defined by (6.29).

as shown in (6.19). To determine the endpoint $x(t)$ of a sample path of free diffusion one creates a chain of random numbers, i.e., a random walk,

$$
\begin{aligned}
x(t = t_N) &= \tilde{r}_N(\ldots \tilde{r}_1(\tilde{r}_0(x_0, t_0), t_1) \ldots, t_N) \\
&= \sqrt{2\,D\,\Delta t}\, \sum_{k=1}^{N} r_k \ .
\end{aligned}
\tag{6.29}
$$

Figure 6.1 displays an ensemble of 1000 such paths, each path being $N = 100$ steps long. The trajectories start at $x = 0$ and proceed towards the rear, as indicated by the time axis. $D = 1$ defines the relation between temporal and spatial units. Ten paths are displayed in black to examplify the behavior of single random walks. The other 990 paths are shown as a grey background. Note the parabolic shape of the trajectory distribution in time. This property, the broadening of the standard deviation of the trajectory distribution proportional to $\sqrt{t}$ was derived in (2.51). In the rear of the figure is a bin count of all trajectory locations at $t = 1$. The solid line imposed on the bar chart represents the theoretical solution according to equation (6.28) with $\Delta t = t - t_0$.

The paths of (6.29) can be used to determine the expectation value $\bar{q}(t|x_0, t_0)$ of an observable Q at time $t = t_N$ as described in (6.10) and (6.20). Obviously such a sampling of an observable value can only be done with a finite ensemble of trajectories. A statistical error in the result is inevitable. Hence the question: how large is the statistical error?

Assume we know the probability $p(x, t|x_0, t_0)$. The exact expectation value $\langle q(t|x_0, t_0) \rangle$ is then given by

$$
\Big\langle q(t|x_0, t_0) \Big\rangle = \int_{\Omega} dx \; q(x)\, p(x, t|x_0, t_0) \ .
\tag{6.30}
$$

One can rewrite (6.30) in terms of a probabilty distribution $\tilde{p}(q, t|x_0, t_0)$ that does not depend on x but on the observable value q.

$$\left\langle q(t|x_0, t_0) \right\rangle \;=\; \int_\Omega dq \; q \; \underbrace{\frac{\partial x(q)}{\partial q} \; p(x(q), t|x_0, t_0)}_{\tilde{p}(q, t|x_0, t_0)} \; . \tag{6.31}$$

With respect to $\tilde{p}(q, t|x_0, t_0)$ we can then express the exact average (6.31) and the variance of the observable value $q(t|x_0, t_0)$ in terms of cumulants.

$$\left\langle q(t|x_0, t_0) \right\rangle \;=\; \left\langle\!\!\left\langle q(t|x_0, t_0) \right\rangle\!\!\right\rangle , \tag{6.32}$$

$$\left\langle \left(q(t|x_0, t_0) \;-\; \left\langle q(t|x_0, t_0) \right\rangle \right)^2 \right\rangle \;=\; \left\langle\!\!\left\langle q^2(t|x_0, t_0) \right\rangle\!\!\right\rangle . \tag{6.33}$$

The variance (6.33) is the variance of single sample readings of an observable Q. Equation (6.33) does not apply to an expectation value $\bar{q}(t|x_0, t_0)$, which is the average of an ensemble of samples. Nevertheless, denoting the outcome of an i-th reading by $q^{(i)}(t|x_0, t_0)$ one can express the expectation value according to (6.20)

$$\bar{q}(t|x_0, t_0) \;=\; \frac{1}{M} \sum_{i=1}^{M} q^{(i)}(t|x_0, t_0) \; . \tag{6.34}$$

The second order cumulant of (6.34) renders

$$\left\langle\!\!\left\langle \bar{q}^2(t|x_0, t_0) \right\rangle\!\!\right\rangle \;=\; \left\langle\!\!\left\langle \left(\frac{1}{M} \sum_{i=1}^{M} q^{(i)}(t|x_0, t_0) \right)^2 \right\rangle\!\!\right\rangle$$

$$\;=\; \frac{1}{M^2} \left\langle\!\!\left\langle \left(\sum_{i=1}^{M} q^{(i)}(t|x_0, t_0) \right)^2 \right\rangle\!\!\right\rangle . \tag{6.35}$$

Since every $q^{(i)}(t|x_0, t_0)$ stems from an independent trajectory sample one can apply (2.44) and we can write

$$\left\langle\!\!\left\langle \bar{q}^2(t|x_0, t_0) \right\rangle\!\!\right\rangle \;=\; \frac{1}{M^2} \sum_{i=1}^{M} \left\langle\!\!\left\langle \left(q^{(i)}(t|x_0, t_0) \right)^2 \right\rangle\!\!\right\rangle . \tag{6.36}$$

Every sample $q^{(i)}(t|x_0, t_0)$ should also exhibit the same variance (6.33) so that we finally obtain

$$\left\langle\!\!\left\langle \bar{q}^2(t|x_0, t_0) \right\rangle\!\!\right\rangle \;=\; \frac{1}{M^2} \sum_{i=1}^{M} \left\langle\!\!\left\langle q^2(t|x_0, t_0) \right\rangle\!\!\right\rangle$$

$$\;=\; \frac{1}{M} \left\langle\!\!\left\langle q^2(t|x_0, t_0) \right\rangle\!\!\right\rangle . \tag{6.37}$$

Hence, the variance of the average of M samples is about $1/M$ times smaller than the variance of a single sample. Consequently the standard deviation of the expectation value decreases with $1/\sqrt{M}$.

To finally determine the statistical error of an expectation value $\bar{q}(t|x_0, t_0)$ given by the standard deviation $\sqrt{\left\langle\!\!\left\langle \bar{q}^2(t|x_0, t_0) \right\rangle\!\!\right\rangle}$ one has to provide a value for the cumulant $\left\langle\!\!\left\langle q^2(t|x_0, t_0) \right\rangle\!\!\right\rangle$ in (6.37). An

estimate for the upper limit of this variance is sufficient in most cases. One can provide an estimate either with the help of some analytical approximation or by simply determining the variance of an ensemble of $\tilde{M}$ samples $q^{(i)}(t|x_0, t_0)$ according to

$$\left\langle\!\!\left\langle q^2(t|x_0, t_0) \right\rangle\!\!\right\rangle \quad \approx \quad \frac{1}{\tilde{M} - 1} \sum_{i=1}^{\tilde{M}} \left(q^{(i)}(t|x_0, t_0) - \bar{q}(t|x_0, t_0) \right)^2 . \tag{6.38}$$

To examplify the tools just introduced we will consider a bin count. For a bin count one measures the probability $q_{[a,b]}$ to find a trajectory end point within a given interval $[a, b]$, called bin. The sensitivity function $q(x)$ for a single bin reaching from a to b is $q_{[a,b]}(x) = \Theta(x - a) - \Theta(x - b)$[1]. One can determine the expectation value $\bar{q}_{[a,b]}(t|x_0, t_0)$ with the help of (6.15), (6.20) and (6.29)

$$\begin{aligned} \bar{q}_{[a,b]}(t|x_0, t_0) &= \int_\Omega dx\ q_{[a,b]}(x)\ p(x, t|x_0, t_0) \\ &\approx \frac{1}{M} \sum_{l=1}^{M} q_{[a,b]} \left(\sqrt{2\,D\,\Delta t} \sum_{k_l=1}^{N} r_{k_l} \right) . \end{aligned} \tag{6.39}$$

Performing calculation (6.39) for an array of adjacent bins one can approximate a probability density distribution $p(\boldsymbol{x}, t|\boldsymbol{x}_0, t_0)$ as shown in the rear of Figure 6.1. For that purpose one takes the expectation value $\bar{q}_{[a,b]}(t|x_0, t_0)$ of each bin and divides it by the base length $|b - a|$. One thereby obtains an estimate for the probability density between a and b

$$\begin{aligned} p(x \in [a, b], t|x_0, t_0) &\approx \bar{p}_{[a,b]}(t|x_0, t_0) \\ &= \frac{\bar{q}_{[a,b]}(t|x_0, t_0)}{|b - a|} . \end{aligned} \tag{6.40}$$

How much confidence can we have in a probability density distribution determined through (6.40)? There are two precision objectives to consider. First, one would like to have a sufficient spatial resolution. The bin size should be smaller than the spatial features of the probability distribution $p(x, t|x_0, t_0)$. This can be achieved by implementing a grid with many tiny bins; the smaller the bin, the better. This however is counteracting the second objective. The statistical error of a probability density within a bin increases as the bin size decreases. Thus, one has to balance these two objectives as we will do in the following calculation.

We will focus our attention on a bin $[a, b]$. The spatial resolution res_s of a bin count based on bins like $[a, b]$ is given by the bin size in relation to the relevant diffusion domain Ω

$$res_s = \frac{|a - b|}{|\Omega|} . \tag{6.41}$$

One can define a resolution of the probability density res_p in a similar fashion. Let $\Delta\bar{p}_{[a,b]}(t|x_0, t_0)$ be the standard deviation of the probability density in bin $[a, b]$. One can view this standard deviation $\Delta\bar{p}_{[a,b]}(t|x_0, t_0)$ as the analog to the bin size $|a - b|$. The relation between the standard deviation $\Delta\bar{p}_{[a,b]}(t|x_0, t_0)$ and the size $|p(\Omega)|$ of the overall range of probabilty density values in a distribution would then define the resolution res_p. Hence

$$res_p = \frac{\Delta\bar{p}_{[a,b]}(t|x_0, t_0)}{|p(\Omega)|} . \tag{6.42}$$

---

[1] $\Theta(x)$ represents Heaviside's step function: $\Theta(x) = 0$ for $x < 0$, and $\Theta(x) = 1$ for $x > 0$.

To optimize a bin count one has to balance the resolutions res_s and res_p. We thus assume

$$res_s \quad \approx \quad res_p \, . \tag{6.43}$$

Out of this equation we can derive the sample number M needed to achieve the desired precision goal.

The sample number M enters equation (6.43) via (6.42) and $\Delta \bar{p}_{[a,b]}(t|x_0,t_0)$. Starting with (6.40) one can derive

$$\begin{aligned}
\Delta \bar{p}_{[a,b]}(t|x_0,t_0) &= \sqrt{\left\langle\!\!\left\langle \bar{p}^2_{[a,b]}(t|x_0,t_0) \right\rangle\!\!\right\rangle} \\[2mm]
&= \sqrt{\frac{\left\langle\!\!\left\langle p^2_{[a,b]}(t|x_0,t_0) \right\rangle\!\!\right\rangle}{M}} \\[2mm]
&= \sqrt{\frac{\left\langle\!\!\left\langle q^2_{[a,b]}(t|x_0,t_0) \right\rangle\!\!\right\rangle}{M\, |a-b|^2}} \, .
\end{aligned} \tag{6.44}$$

$\left\langle\!\!\left\langle q^2_{[a,b]}(t|x_0,t_0) \right\rangle\!\!\right\rangle$ can be approximated assuming $\left\langle q_{[a,b]}(t|x_0,t_0) \right\rangle$ to be equal $\bar{q}_{[a,b]}(t|x_0,t_0)$.

$$\begin{aligned}
\left\langle\!\!\left\langle q^2_{[a,b]}(t|x_0,t_0) \right\rangle\!\!\right\rangle &= \left\langle \left(q_{[a,b]}(t|x_0,t_0) - \left\langle q_{[a,b]}(t|x_0,t_0) \right\rangle \right)^2 \right\rangle \tag{6.45} \\[2mm]
&\approx \left\langle \left(q_{[a,b]}(t|x_0,t_0) - \bar{q}_{[a,b]}(t|x_0,t_0) \right)^2 \right\rangle \tag{6.46} \\[2mm]
&= \left(1 - \bar{q}_{[a,b]}(t|x_0,t_0) \right)^2 \bar{q}_{[a,b]}(t|x_0,t_0) \; + \\
&\quad\; \left(0 - \bar{q}_{[a,b]}(t|x_0,t_0) \right)^2 \left(1 - \bar{q}_{[a,b]}(t|x_0,t_0) \right) \tag{6.47} \\[2mm]
&= \bar{q}_{[a,b]}(t|x_0,t_0) \left(1 - \bar{q}_{[a,b]}(t|x_0,t_0) \right) \tag{6.48}
\end{aligned}$$

Inserting (6.48) back into (6.44) one obtains

$$\Delta \bar{p}_{[a,b]}(t|x_0,t_0) \quad = \quad \sqrt{\frac{\bar{q}_{[a,b]}(t|x_0,t_0) \left(1 - \bar{q}_{[a,b]}(t|x_0,t_0) \right)}{M\, |a-b|^2}} \tag{6.49}$$

Implementing (6.49) in (6.42) and (6.43) and solving for M we derive

$$M \quad = \quad \bar{q}_{[a,b]}(t|x_0,t_0) \left(1 - \bar{q}_{[a,b]}(t|x_0,t_0) \right) \left(\frac{|\Omega|}{|a-b|^2\, |p(\Omega)|} \right)^2 \, . \tag{6.50}$$

One can use equation (6.50) to estimate the number of particles needed in a Brownian dynamics simulation when creating probability distributions via a bin count. In Figure 6.1 we had to consider the parameters $|\Omega| = 6$, $\Delta x = 0.3$, $|p(\Omega)| = 0.4$ and $\bar{q}_{[a,b]} = \Delta x\, \bar{p}_{[a,b]} \approx 0.04$. With these numbers equation (6.50) renders $M = 1067$ which is roughly the number of trajectories used in our example. Unfortunately many interesting simulations require much larger M and thus tremendous computational resources.

6.5   Reflective Boundary Conditions

So far in this chapter we have considered solely Brownian dynamics with boundaries at $x \rightarrow \pm\infty$. We now seek to account for the existence of refelctive boundaries at finite positions in the diffusion domain. For the purspose of a numerical Brownian dynamics description we divide

again teh evolution of teh probability function into many small time intervals, assuming that the corresponding Δx and Δt values are small such that conditions (6.6) and (6.7) are satisfied. Furthermore we now assume, that the average spatial increment Δx of a simulated trajectory is minute compared to the spatial geometry of the diffusion domain and its reflective boundary. In this case a stochastic trajectory will most likely encounter not more than a single boundary segment in each time interval. It will be permissible, therefore, to consider only one boundary segment at a time. Furthermore, we approximate these boundary segments by planes, which is appropriate as long as the curvature of the boundary is small in comparison to Δx.

Under all these conditions one can again provide an approximate analytical solution $p(\boldsymbol{x}, t_0 + \Delta t | \boldsymbol{x}_0, t_0)$ for a single simulation step. One can then use this solution to construct an adequate numerical simulation over longer time intervals.

As stated, we assume refelective boundaries governed by the boundary condition (4.24)

$$\hat{\boldsymbol{a}}(\boldsymbol{x}) \cdot \boldsymbol{\mathcal{J}} \; p(\boldsymbol{x}, t | \boldsymbol{x}_0, t_0) \;\; = \;\; 0 \;, \quad \boldsymbol{x} \text{ on } \partial\Omega_i \;, \tag{6.51}$$

where $\hat{\boldsymbol{a}}(\boldsymbol{x})$ denotes the normalized surface vector of the planar boundary segment. One derives an analytical solution for $p(\boldsymbol{x}, t | \boldsymbol{x}_0, t_0)$ in the present case by emulating a mirror image of a diffusing particle behind the planar boundary segment so that the flow of particles and the flow of mirror particles through the boundary segment cancel each other to satisfy (6.51). This is established through the probability

$$
\begin{aligned}
p(\boldsymbol{x}, t_0 + \Delta t | \boldsymbol{x}_0, t_0) \;\; = \;\; & \left(\frac{1}{\sqrt{2\pi \, [\mathbf{B} \cdot \mathbf{B}^{\mathsf{T}}] \, (\boldsymbol{x}_0, t_0) \, \Delta t}} \right)^n \exp\left[-\frac{(\boldsymbol{x} - \boldsymbol{x}_0 - \boldsymbol{A}(\boldsymbol{x}_0, t_0) \, \Delta t)^2}{2 \, [\mathbf{B} \cdot \mathbf{B}^{\mathsf{T}}] \, (\boldsymbol{x}_0, t_0) \, \Delta t} \right] \\
& + \left(\frac{1}{\sqrt{2\pi \, [\mathbf{B} \cdot \mathbf{B}^{\mathsf{T}}] \, (\boldsymbol{x}_0, t_0) \, \Delta t}} \right)^n \exp\left[-\frac{(\boldsymbol{x} - \mathcal{R}_{\partial\Omega}[\boldsymbol{x}_0 + \boldsymbol{A}(\boldsymbol{x}_0, t_0) \, \Delta t])^2}{2 \, [\mathbf{B} \cdot \mathbf{B}^{\mathsf{T}}] \, (\boldsymbol{x}_0, t_0) \, \Delta t} \right] \;.
\end{aligned}
\tag{6.52}
$$

$\mathcal{R}_{\partial\Omega}$ denotes the operation of reflection at the boundary plane $\partial\Omega$. To perform the reflection operation $\mathcal{R}_{\partial\Omega}$ explicitly one splits every position vector $\boldsymbol{x}$ into two components, one parallel $x_\parallel$ and one orthogonal $x_\perp$ to the planar boundary $\partial\Omega$. If $\boldsymbol{b} \in \partial\Omega$ one can express the operation of reflection as

$$x_\parallel \quad \overset{\mathcal{R}_{\partial\Omega}}{\longmapsto} \quad x_\parallel \tag{6.53}$$

$$x_\perp \quad \overset{\mathcal{R}_{\partial\Omega}}{\longmapsto} \quad 2\, b_\perp \; - \; x_\perp \;. \tag{6.54}$$

With this notation one can write boundary condition (6.51) as

$$\left(\frac{[\mathbf{B} \cdot \mathbf{B}^{\mathsf{T}}] \, (\boldsymbol{x}, t)}{2} \, \partial_{x_\perp} \; - \; \boldsymbol{A}(\boldsymbol{x}, t) \right) \; p(\boldsymbol{x}, t_0 + \Delta t | \boldsymbol{x}_0, t_0) \, \Bigg|_{\boldsymbol{x} \in \partial\Omega} \;\; = \;\; 0 \;. \tag{6.55}$$

and one can easily verify that equation (6.52)

$$
\begin{aligned}
p(\boldsymbol{x}, t | \boldsymbol{x}_0, t_0) \;\; = \;\; & \left(\frac{1}{\sqrt{2\pi \, [\mathbf{B} \cdot \mathbf{B}^{\mathsf{T}}] \, (\boldsymbol{x}_0, t_0) \, \Delta t}} \right)^n \left(\exp\left[-\frac{(\boldsymbol{x} - \boldsymbol{x}_0)^2}{4 \, D \, \Delta t} \right] \right. \\
& \left. + \; \exp\left[-\frac{\left(\boldsymbol{x}_\parallel - \boldsymbol{x}_{0\parallel}\right)^2 + (\boldsymbol{x}_\perp + \boldsymbol{x}_{0\perp} - 2\, b_\perp)^2}{2 \, [\mathbf{B} \cdot \mathbf{B}^{\mathsf{T}}] \, (\boldsymbol{x}_0, t_0) \, \Delta t} \right] \right)
\end{aligned}
\tag{6.56}
$$

is a solution of the diffusion equation which obeys (6.55).

The function on the r.h.s. of (6.56) describes a Wiener process which is modified, in that the endpoint of the Gaussian distribution which reaches across the boundary $\partial\Omega$ is 'reflected' back into the domain Ω. The modified Wiener process is therefore defined as follows

$$
\boldsymbol{x}(t+\Delta t) \;=\; \begin{cases} \boldsymbol{x}(t) \;+\; \sqrt{2\,D\,\Delta t}\;\boldsymbol{r}(t) & \text{, if } \boldsymbol{x}(t) \;+\; \sqrt{2\,D\,\Delta t}\;\boldsymbol{r}(t) \;\in\; \Omega \\[2mm] \mathcal{R}_{\partial\Omega}\left[\boldsymbol{x}(t) \;+\; \sqrt{2\,D\,\Delta t}\;\boldsymbol{r}(t)\right] & \text{, if } \boldsymbol{x}(t) \;+\; \sqrt{2\,D\,\Delta t}\;\boldsymbol{r}(t) \;\notin\; \Omega \end{cases} \tag{6.57}
$$

Whenever $\boldsymbol{x}(t+\Delta t)$ reaches outside the domain Ω the actual value of the coordinate $\boldsymbol{x}(t+\Delta t)$ is readjusted according to the rules set by Eq. (6.57).